Angiotensin-Converting Enzyme 3 (ACE3) Protects Against Pressure Overload-Induced Cardiac Hypertrophy

Chang-Jiang Yu, PhD;* Liang-Liang Tang, PhD;* Chen Liang, MS; Xiao Chen, MS; Shu-Ying Song, MS; Xiao-Qing Ding, MS; Kun-Yu Zhang, MS; Bin-Lin Song, BS; Dan Zhao, PhD; Xue-Yong Zhu, BS; Hong-Liang Li, MD, PhD; Zhi-Ren Zhang, MD, PhD

Background—Angiotensin-converting enzyme 3 (ACE3) is a recently defined homolog of ACE. However, the pathophysiological function of ACE3 is largely unknown. Here, we aim to explore the role of ACE3 in pathological cardiac hypertrophy.

Methods and Results—Neonatal rat cardiomyocytes (NRCMs) with gain and loss of function of ACE3 and mice with global knockout or cardiac-specific overexpression of ACE3 were used in this study. In cultured cardiomyocytes, ACE3 conferred protection against angiotensin II (Ang II)-induced hypertrophic growth. Cardiac hypertrophy in mice was induced by aortic banding (AB) and the extent of hypertrophy was analyzed through echocardiographic, pathological, and molecular analyses. Our data demonstrated that ACE3-deficient mice exhibited more pronounced cardiac hypertrophy and fibrosis and a strong decrease in cardiac contractile function, conversely, cardiac-specific ACE3-overexpressing mice displayed an attenuated hypertrophic phenotype, compared with control mice, respectively. Analyses of the underlying molecular mechanism revealed that ACE3-mediated protection against cardiac hypertrophy by suppressing the activation of mitogen-activated protein kinase kinase (MEK)-regulated extracellular signal-regulated protein kinase (ERK1/2) signaling, which was further evidenced by the observation that inhibition of the MEK-ERK1/2 signaling by U0126 rescued the exacerbated hypertrophic phenotype in ACE3-deficient mice.

Conclusions—Our comprehensive analyses suggest that ACE3 inhibits pressure overload-induced cardiac hypertrophy by blocking the MEK-ERK1/2 signaling pathway. (*J Am Heart Assoc*. 2016;5:e002680 doi: 10.1161/JAHA.115.002680)

Key Words: angiotensin-converting enzyme 3 • cardiac hypertrophy • ERK1/2 • MEK1/2 • signaling pathway

C ardiac hypertrophy develops as an adaptive response to an increased workload induced by diverse pathological stimuli, eg, hypertension, aortic stenosis, and valvular diseases.[1] Cardiac hypertrophy is usually characterized by the enlargement of cardiomyocytes, an increase in protein synthesis, the reorganization of sarcomeres and the reactivation of the fetal gene program. Although the initial hypertrophic phase is indeed compensatory to maintain cardiac output, the beneficial effects are contravened by sustained pathological hypertrophy, which eventually results in malignant arrhythmia, heart failure, and sudden death.[2–4] Numerous signal transduction pathways have been studied in the hypertrophic process, such as the PI3K/AKT/GSK3β pathway, the calcineurin/nuclear factor of activated T cells (NFAT) pathway, and the mitogen-activated protein kinase (MAPK) pathway.[5–7] However, the underlying mechanisms during the development of cardiac hypertrophy are rather complicated and remain to be completely discovered.

Recently, a new component of the ACE family was identified and characterized through bioinformatics analyses, termed ACE3.[8] ACE3 has one single functional domain (the zinc-binding motif), and the most important catalytic Glu in this motif is substituted by Gln, which indicates that ACE3 should lack the catalytic activity as a zinc metalloprotease. To date, the only known biological function of ACE3 is that it functions as an IZUMO-interacting protein (IZUMO is an essential sperm protein for sperm-egg fusion) involved in the acrosome reaction in sperm.[9] In consideration of the critical roles of the ACE3 homologs, ACE, and ACE2 that played in different pathogeneses of cardiovascular diseases, we are interested to know whether ACE3 can also function as a

regulator in cardiovascular diseases, especially the development of cardiac hypertrophy and heart failure.

In this study, we first demonstrated that the expression of ACE3 was downregulated in both cardiomyocytes and mouse hearts subjected to hypertrophic stress. Moreover, compared with the controls, ACE3-deficient mice developed more severe cardiac hypertrophy, fibrosis, and dysfunction upon chronic pressure overload, whereas the opposite effects occurred in ACE3-overexpressing mice. At the molecular level, we identified that the MEK-ERK1/2 signaling pathway was a crucial target of ACE3 in the regulation of pathological cardiac hypertrophy. Furthermore, inhibition of the MEK-ERK1/2 signaling with U0126 rescued cardiac dysfunction in ACE3-knockout mice.

Methods

Reagents

Antibodies specific to the following proteins were purchased from Cell Signaling Technology (Danvers, MA, USA) and used in western blot experiments: phospho-MEK1/2$^{Ser32/36}$ (9154, 1:1000 dilution); total-MEK1/2 (9122, 1:1000 dilution); phospho-ERK1/2$^{Thr202/Tyr204}$ (4370, 1:1000 dilution); total-ERK1/2 (4695, 1:1000 dilution); phospho-JNK1/2$^{Thr183/Tyr185}$ (4668, 1:1000 dilution); total-JNK (9258, 1:1000 dilution); phospho-P38$^{Thr180/Tyr182}$ (4511, 1:1000 dilution); and total-P38 (9212, 1:1000 dilution). Antibodies specific to the following proteins were purchased from Santa Cruz Biotechnology (Dallas, TX): ANP (sc20158, 1:200 dilution) and β-MHC (sc53090, 1:200 dilution). Anti-GAPDH (MB001, 1:10000 dilution) was purchased from Bioworld Technology (Harrogate, UK). Anti-ACE3 (BAM-73-006-EX, 1:500 dilution) was purchased from COSMO BIO Co, Ltd (Tokyo, Japan). The BCA protein assay kit was purchased from Pierce (Rockford, IL). Peroxidase-conjugated secondary antibodies were purchased from Jackson ImmunoResearch Laboratories (West Grove, PA) and used for visualization. Unless otherwise noted, cell culture reagents and all other reagents were obtained from Sigma (St. Louis, MO).

Neonatal Rat Cardiomyocyte Culture and Recombinant Adenoviral Vectors

Primary cultures of neonatal rat cardiac myocytes were prepared as described previously.[10,11] In detail, neonatal (1- to 2-day-old) Sprague-Dawley rats were sacrificed by swift decapitation according to Guide for the Care and Use of Laboratory Animals published by the United States National Institutes of Health. Then, ventricle tissues of these mice were finely minced and dissociated into individual cardiomyocytes with multiple rounds of enzymatic digestion in phosphate buffered saline (PBS) containing 0.03% trypsin and 0.04% type II collagenase. After removal of non-myocytes, the harvested cardiomyocytes were seeded into 0.1% gelatin-coated 6-well culture plates at a density of 1×10^6 cells/well in DMEM/F12 containing 10% fetal bovine serum (FBS), 100 U/mL penicillin/100 mg per mL streptomycin (Gibco, 15140), and 0.1 mmol/L BrdU (5-bromo-2′-deoxyuridine) to inhibit the growth of non-myocytes. After 48 hours of incubation, the culture medium was replaced by serum-free DMEM/F12 for another 12 hours of cultivation before treatment with angiotensin II (Ang II, 1 μmol/L) to induce hypertrophy. To overexpress ACE3, full length rat ACE3 cDNA under the control of the cytomegalovirus (CMV) promoter was cloned into a replication-defective adenoviral vector. A similar adenoviral vector containing green fluorescent protein (GFP) was used as a control. To knock down ACE3 expression, rat short hairpin ACE3 (shACE3) constructs were ordered from SABiosciences (KR65067G), and AdshACE3 adenovirus was generated subsequently. AdshRNA was used as the non-targeting control.

Immunofluorescence Analysis

Immunofluorescence analysis was performed following the standard immunofluorescence staining procedures. Briefly, after the NRCMs were infected with the indicated recombinant adenoviruses and treated with hypertrophic stimuli, the cardiomyocytes were fixed with 100% methanol for 20 minutes and permeabilized with 0.1% Triton X-100 in PBS for 40 minutes. Then, the cells were blocked with 10% BSA in PBS followed by staining with α-actinin (1:100 dilution). The cells were visualized using a fluorescence microscope (Olympus) and measured using Image-Pro Plus 6.0 software.

Experimental Mouse Models and Surgical Procedure

All animal experimental protocols were approved by the Institutional Animal Care and Use Committee of Cancer Hospital of Harbin Medical University, and were conducted in accordance with the National Institutes of Health (NIH) Guide for the Care and Use of Laboratory Animals.

Generation of ACE3-knockout (ACE3-KO) mice

Global ACE3-KO mice (B6;129-Ace3<tm1Osb>; Stock No. RBRC04138) were purchased from the RIKEN BioResource Center. All the mice used in our animal experiments were C57BL/6J background. To rule out the potential effects of the mixed genetic background of ACE3-KO mice (B6;129 background) during our experiments, the ACE3-KO mice (B6;129 background) were crossed with C57BL/6J mice to produce the F1 generation (ACE3 heterozygotes), which was back-

crossed with the C57BL/6J strain to obtain the F2 generation (ACE3 heterozygotes), and then further backcrossed to the C57BL/6J background until the F9 generation (ACE3 heterozygous). Male and female mice of the F9 generation were crossed with each other to produce ACE3-KO mice in a pure C57BL/6J background.

Production of ACE3-transgenic (ACE3-TG) mice

We initially generated transgenic mice carrying a construct of CAG gene promoter-loxP-CAT gene-loxP-mACE3 region (designated CAG-CAT-mACE3 transgenic mice), which was designed to induce mouse ACE3 expression by Cre-mediated recombination. The CAG-CAT-mACE3 transgenic mice developed normally and showed no abnormalities. Founder transgenic mice were identified by tail DNA amplification. The PCR primers for transgenic detection, CAG-For (5′-CCCCCTGAAC CTGAAACATA-3′) and ACE3-Rev (5′-TTCTGCTTGGTGATGTT GGT-3′), yielded a 551-bp product. To induce ACE3 expression specifically in the heart, the CAG-CAT-mACE3 transgenic mice (strain C57BL/6J) were bred with α-MHC-MerCreMer transgenic mice (Myh6-cre/Esr1, Jackson Laboratory, 005650) that carried the Cre gene under the control of the α-MHC gene promoter to generate CAG-CAT-mACE3/α-MHC-MerCreMer double-transgenic mice. To generate cardiac-specific conditional ACE3 transgenic mice, Cre-mediated recombination of loxP alleles (CAT gene excision from the construct) was induced by an intraperitoneal injection of tamoxifen (80 mg/kg per day) for 5 consecutive days. The CAG-CAT-mACE3/α-MHC-MerCreMer mice without tamoxifen administration (CAMC) littermates served as the control group.

Male mice aged 8 to 10 weeks with body weights of 24 to 27 g were used in these experiments. All animals were housed at constant (22°C) temperature on controlled light cycles (12-hour light/dark) with ad libitum access to food and water. All animal experiments were performed by an experimenter who was blinded to the animal genotypes.

Aortic banding

Aortic banding (AB) was performed by following previously described methods.[12–14] Briefly, age- and sex-matched mice were anesthetized with sodium pentobarbital (50 mg/kg, i.p., Sigma), and they did not display any foot reflex. Then, the thoracic aorta was identified by carefully blunting dissection at the second intercostal space after the left chest of each mouse was opened. Immediately, a small piece of a 7-0 nylon suture was placed around the transverse aorta, and tied around a 27G (for body weights of 24–25 g) or 26G (for body weights of 26–27 g) blunt needle to produce a 65% to 70% constriction. The needle was slightly removed before suturing the thoracic cavity. When the AB was completely performed,

Doppler analysis was used to confirm adequate constriction of the aorta. A sham operation was performed in which the same surgical procedures were performed without constricting the aorta.

Treatment of Mice With U0126

U0126, a MAPK kinase (MEK) 1/2 inhibitor, was purchased from Cell Signaling Technology (#9903, Beverly, MA) and dissolved in dimethyl sulfoxide (DMSO) to a concentration of 0.1 mg/mL. U0126 suspension was freshly prepared and administered at a constant volume of 1 mL/100 g body weight every 3 days (1 mg/kg per 3 days, i.p.). The control group for this experiment was given the same volume of mixture without U0126.

Echocardiographic Experiments

Cardiac function was evaluated in anesthetized (1.5–2% isoflurane) mice at the indicated time, using a MyLab 30CV ultrasound (Biosound Esaote Inc., Genova, Italy) equipped with a 15-MHz linear transducer.[14] The heart was imaged in short-axis views with a depth setting of 2 cm. The cursor was positioned perpendicular to the interventricular septum and posterior wall of the left ventricular (LV) at the level of the mid-papillary muscle, with tracing with a sweep speed of 50 mm/s for measurement of LV end-systolic diameter (LVESd) and LV end-diastolic diameter (LVEDd). The percentage of fractional shortening (FS) was calculated with the following formula: FS (%)=(LVEDd−LVESd)/LVEDd×100%.

Histological Analysis

The hearts were excised from animals sacrificed 4 weeks after AB or sham operation. After being arrested with 10% potassium chloride solution, the hearts were washed with PBS and fixed in 10% formalin. Paraffin-embedded hearts were sectioned transversely at 5 μm, and the left and right ventricles were presented clearly. The sections were loaded on slides and prepared for the following experiments. The sections were stained with hematoxylin and eosin (H&E) to determine the cross-sectional area of myocytes and with picrosirius red (PSR) for the collagen deposition. In addition, sections were stained with FITC-conjugated wheat germ agglutinin (WGA; Invitrogen) to identify the membrane and with DAPI to stain the nuclei to enhance the visual effects of cross-sectional area (CSA) of cardiomyocytes. The CSA of a single myocyte and the volume of fibrillar collagen were visualized by microscopy and measured with a quantitative digital image analysis system (Image-Pro Plus 6.0).

Western Blotting

Whole-cell lysates were extracted from ventricles and primary cells in lysis buffer. Protein concentrations were determined with a BCA Protein Assay Kit (Pierce, CAT: 23225). A total of 50 µg of protein was electrophoresed in 10% SDS–PAGE (Invitrogen) and transferred to polyvinylidene fluoride (PVDF) membranes (Millipore). The membranes were blocked with 5% fat-free milk, followed by incubation with primary antibodies over night at 4°C. Subsequently, the membranes were incubated with appropriate peroxidase-conjugated secondary antibodies for 60 minutes at room temperature. The immunoreactive proteins were visualized using the enhanced chemiluminescence (ECL) detection system (170-5061, Bio-Rad). Signals were detected and quantified by using Bio-Rad ChemiDoc™ XRS⁺ (Bio-Rad). The specific protein expression levels were normalized to the levels of GAPDH on the same PVDF membrane.

Real-Time PCR

According to the manufacturer's protocol, total RNA was extracted from cultured primary NRCMs or frozen mouse cardiac tissues using TRIZol (Invitrogen). To generate cDNA, 2 µg of total RNA was reverse transcribed using the Transcriptor First Strand cDNA Synthesis Kit (Roche). Then, quantitative RNA amplification was performed using a Light-Cycler 480 Real-Time PCR Systems (Roche) with SYBR Green Master Mix (Roche) and the products were routinely checked by using dissociation curve software. Transcript quantities were compared by normalizing the amount of detected mRNA against endogenous control glyceraldehyde-3-phosphate dehydrogenase (GAPDH). The primers used for Real-time PCR are shown in Table.

Statistical Analyses

The data are expressed as mean±SEM. All statistical analyses were performed with SPSS software (version 20.0; IBM Corp, Armonk, NY). Normal distribution was tested for all data sets using the Shapiro-Wilkison normality test. For normally distributed data, comparison between 2 groups was performed using the unpaired Student t test and differences among groups were calculated for significance by using 1-way ANOVA, followed by Bonferroni post hoc test (equal variances assumed) or Tamhane's T2 post hoc test (equal variances not assumed). Two-way ANOVA was performed to analyze differences by treatment and genotype when we compared 4 groups. For abnormally distributed data, the Mann–Whitney U test or Kruskal–Wallis test were applied to calculate for significance. A value of $P<0.05$ was considered to indicate a statistically significant difference.

Table. The Primers for Real-Time PCR

Primer Name	Sequence
ANP-Rat-Forward	AAAGCAAACTGAGGGCTCTGCTCG
ANP-Rat-Reverse	TTCGGTACCGGAAGCTGTTGCA
BNP-Rat-Forward	CAGCAGCTTCTGCATCGTGGAT
BNP-Rat-Reverse	TTCCTTAATCTGTCGCCGCTGG
β-MHC-Rat-Forward	TCTGGACAGCTCCCCATTCT
β-MHC-Rat-Reverse	CAAGGCTAACCTGGAGAAGATG
ANP-Mouse-Forward	ACCTGCTAGACCACCTGGAG
ANP-Mouse-Reverse	CCTTGGCTGTTATCTTCGGTACCGG
BNP-Mouse-Forward	GAGGTCACTCCTATCCTCTGG
BNP-Mouse-Reverse	GCCATTTCCTCCGACTTTTCTC
β-MHC-Mouse-Forward	CCGAGTCCCAGGTCAACAA
β-MHC-Mouse-Reverse	CTTCACGGGCACCCTTGGA
Collagen I-mouse-Forward	AGGCTTCAGTGGTTTGGATG
Collagen I-mouse-Reverse	CACCAACAGCACCATCGTTA
Collagen III-mouse-Forward	CCCAACCCAGAGATCCCATT
Collagen III-mouse-Reverse	GAAGCACAGGAGCAGGTGTAGA
Fibronectin-mouse-Forward	CCGGTGGCTGTCAGTCAGA
Fibronectin-mouse-Reverse	CCGTTCCCACTGCTGATTTATC
ACE2-Rat-Forward	GAACAGTCCAAGATCGCCCA
ACE2-Rat-Reverse	GTTCTTGTCTGGTGACAGCG

ACE2 indicates Angiotensin-converting enzyme 2; ANP, atrial natriuretic peptide; BNP, brain natriuretic peptide; β-MHC, β-myosin heavy chain; PCR, polymerase chain reaction.

Results

ACE3 Expression Levels are Decreased in Hypertrophic Mouse Hearts

To investigate the potential role of ACE3 in the development of cardiac hypertrophy and heart failure, we first analyzed ACE3 expression in mouse hypertrophic hearts and neonatal rat cardiomyocytes (NRCMs). Western blotting analysis demonstrated that ACE3 expression was significantly downregulated in the hearts of mice subjected to aortic banding (AB) for 4 or 8 weeks (Figure 1A). The ACE3 protein expression levels were reduced by ≈36% and ≈48% in the experimental mouse hearts compared with the sham-operated control hearts after 4 or 8 weeks of AB treatment, respectively. Correspondingly, the decrease in ACE3 was accompanied by increases in the hypertrophic markers atrial natriuretic peptide (ANP) and β-myosin heavy chain (β-MHC). In accordance with these findings in animal experiments, treatment of NRCMs with angiotensin II (Ang II; 1 µmol/L) for 24 or 48 hours to induce hypertrophy resulted in the downregulation of ACE3 and the upregulation of ANP and β-MHC (Figure 1B). These results indicate that ACE3 expression is markedly decreased in pressure overload-induced hypertrophic mouse hearts and in
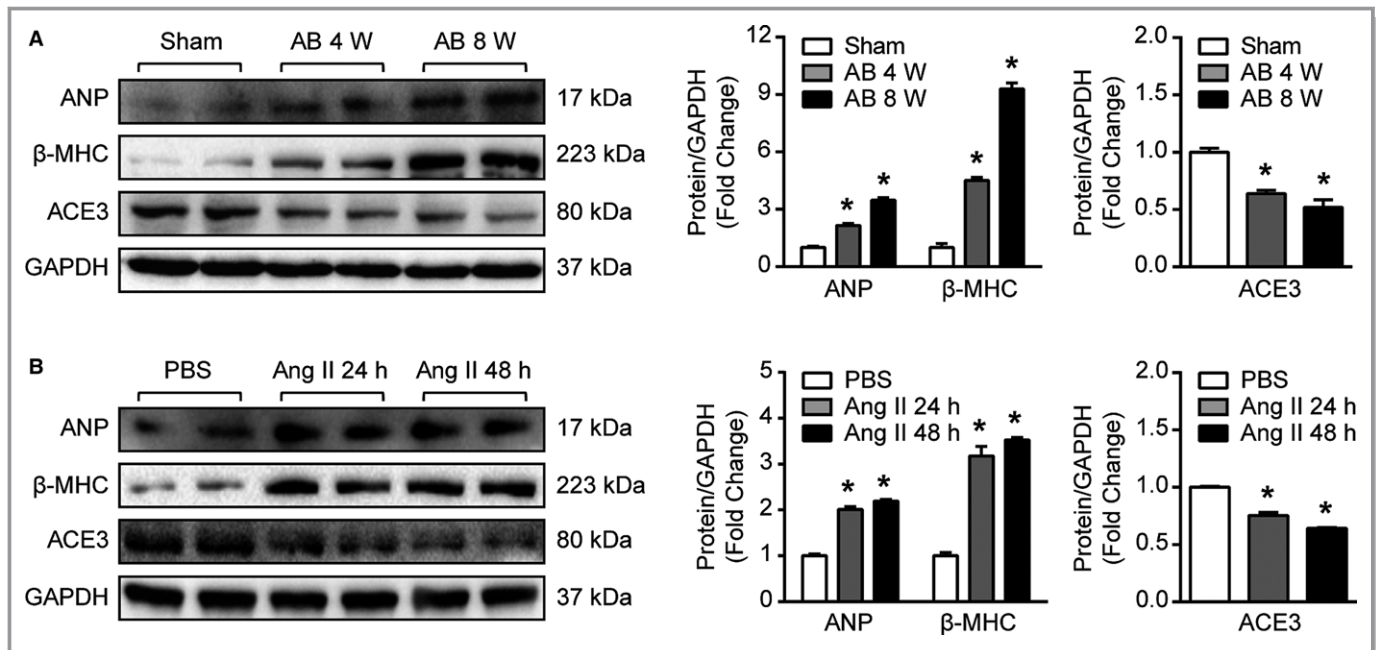
Figure 1. Angiotensin-converting enzyme 3 (ACE3) expression levels are reduced by hypertrophic stimuli. A, Western blot analysis and quantification of atrial natriuretic peptide (ANP), β-myosin heavy chain (β-MHC), and ACE3 in hearts of mice at 4 and 8 weeks after sham or aortic banding (AB) treatment (n=6 mice in each group; *$P<0.05$ vs sham). B, Representative western blots and quantitative results of ANP, β-MHC, and ACE3 in extracts from neonatal rat cardiomyocytes (NRCMs) treated with phosphate buffered solution (PBS) or angiotensin II (Ang II; 1 μmol/L) for 24 and 48 hours (n=6 samples in each group; *$P<0.05$ vs PBS).

Ang II-treated cardiomyocytes, thus suggesting a potential functional role of ACE3 in the process of hypertrophic growth.

ACE3 Attenuates Angiotensin II-Induced Cardiomyocyte Hypertrophy

Next, we performed gain- and loss-of-function studies in NRCMs to investigate the potential function of ACE3 on cardiomyocyte hypertrophy. NRCMs were infected with an adenovirus harboring ACE3 short hairpin RNA (AdshACE3) to reduce the level of ACE3 and full-length ACE3 cDNA (AdACE3) to elevate the level of ACE3, AdshRNA, and AdGFP were infected to serve as negative controls (Figure 2A). At baseline, downregulation or upregulation of ACE3 had no significant effects on the gene expression of ACE2 (Figure 2B). Then, the infected cardiomyocytes were further stimulated with Ang II (1 μmol/L) or with PBS as a control for 48 hours (Figure 2C). The morphology of cardiomyocytes was visualized by immunostaining with the α-actinin-specific antibody. Neither AdshACE3 nor AdACE3 had effects on cardiomyocyte morphology or cell size in the control conditions (PBS). However, AdshACE3 treatment enhanced the Ang II-induced increase in cell surface area (by ≈44%, Figure 2C and 2D), whereas upregulation of ACE3 (AdACE3) attenuated the hypertrophic response to Ang II treatment compared with the response in controls (by ≈42%, Figure 2C and 2E). Consistently, the

expression of the hypertrophic markers ANP, BNP, and β-MHC were further increased in the AdshACE3-infected NRCMs after treatment with Ang II, compared with control groups (Figure 2F). However, AdACE3 infection significantly attenuated the elevated expression of hypertrophic markers in response to Ang II treatment (Figure 2G). Together, these observations indicate that ACE3 is capable of suppressing the hypertrophic response in cardiomyocytes.

Ablation of ACE3 Exhibits an Increased Susceptibility to Pressure Overload-Induced Cardiac Hypertrophy

We have demonstrated the negative effects of ACE3 on cardiomyocyte hypertrophy in vitro. To examine the functional contribution of ACE3 during cardiac hypertrophy in vivo, we used a global ACE3 gene knockout (ACE3-KO) mouse model; western blotting analysis revealed that the ACE3 protein expression in these mice was absent in the heart (Figure 3A). Then, we subjected the mice to AB surgery or sham operation and performed analyses 4 weeks thereafter. Remarkably, 4 weeks after AB surgery, ACE3-KO mice exhibited an enhanced hypertrophic phenotype compared with wild-type (WT) littermates, as indicated by the higher ratios of heart weight to body weight (HW/BW), lung weight (LW) to BW, and HW to tibia length (TL; Figure 3B). In addition, hematoxylin &
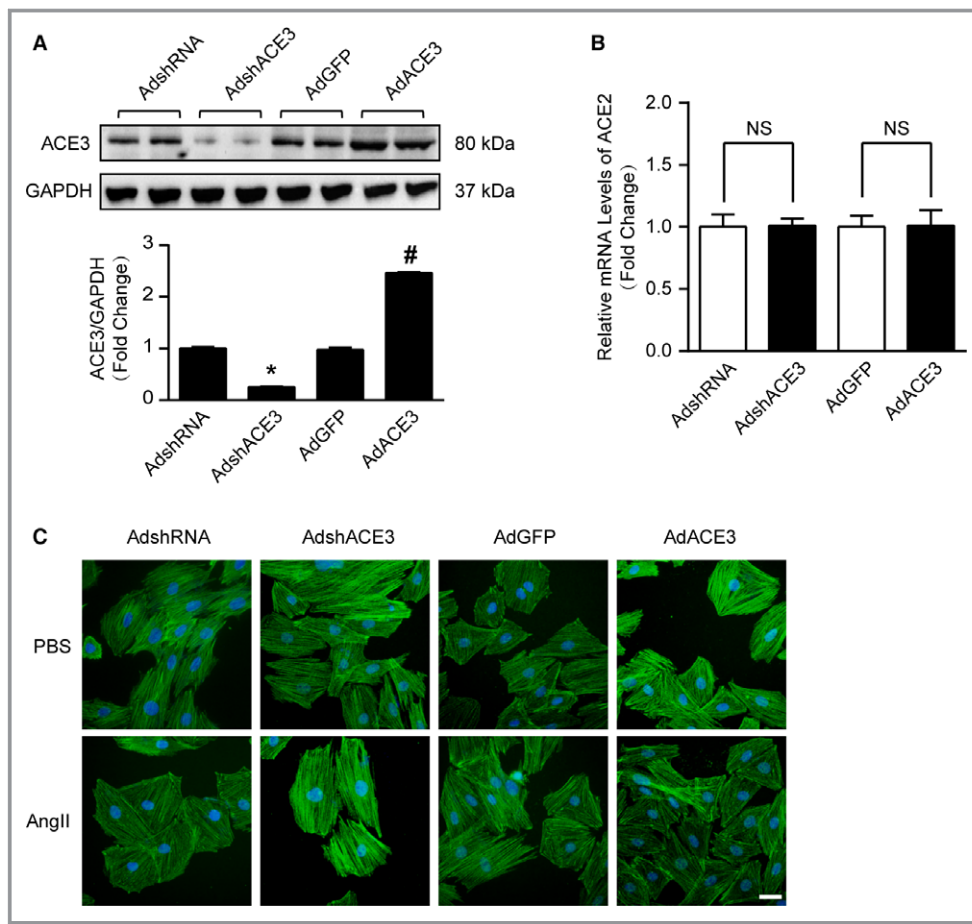
Figure 2. Angiotensin-converting enzyme 3 (ACE3) negatively regulates angiotensin II (Ang II)-induced cardiomyocyte hypertrophy. A, NRCMs infected with AdACE3, AdshACE3, or their respective controls (adenoviral vectors expressing green fluorescent protein [AdGFP] and adenoviral vectors expressing short hairpin ribonucleic acid [AdshRNA]) were analyzed by western blotting. The quantitative results are presented on the right (n=3 independent experiments; *P<0.05 vs AdshRNA or AdGFP). B, Real-time PCR analyses of ACE2 mRNA levels in AdshACE3- and AdACE3-infected NRCMs (n=4 samples in each group; NS, no significant). C, Representative images of cardiomyocytes infected with AdshACE3 or AdACE3 and treated with PBS or Ang II (1 μmol/L) for 48 hours (green, α-actinin; blue, nuclei; scale bars, 20 μm). D and E, Quantification of cell surface area (n=50 cells in each group; *P<0.05 vs AdshRNA/PBS or AdGFP/PBS; #P<0.05 vs AdshRNA/Ang II or AdGFP/Ang II). F and G, Real-time PCR analyses of ANP, brain natriuretic peptide (BNP), and β-MHC mRNA levels in AdshACE3- and AdACE3-infected NRCMs after treatment with either PBS or Ang II for 48 hours (n=4 samples in each group; *P<0.05 vs AdshRNA/PBS or AdGFP/PBS; #P<0.05 vs AdshRNA/Ang II or AdGFP/Ang II).

eosin (H&E) and wheat germ agglutinin (WGA) staining showed a significantly greater ventricular cross-sectional area in the ACE3-KO mice than that in the WT mice after 4 weeks of AB surgery (Figure 3C and 3D), further confirming that ACE3 deficiency promoted the development of pressure overload-induced cardiac hypertrophy. Moreover, echocardiography experiments were performed to estimate the alterations in cardiac contractile function, these measurements (left ventricular end-diastolic diameter [LVEDd], left ventricular end-systolic diameter [LVESd], and fractional shortening [FS]) indicated that the enhanced cardiac hypertrophy in ACE-KO mice compared with WT mice was accompanied by

aggravated left ventricular dysfunction (Figure 3E). Consistently with these morphological and functional alterations, the mRNA levels of the hypertrophic markers ANP, BNP, and β-MHC were significantly higher in the ACE3-KO mice than in controls after 4 weeks of AB treatment (Figure 3H).

Fibrosis is a classical feature of pathological cardiac hypertrophy. Therefore, to further define the effects of ACE3 deficiency on cardiac remodeling, picrosirius red (PSR) staining was used to identify the changes in fibrosis. Our results revealed that both interstitial and perivascular fibrosis were more extensive in ACE3-KO mice than in WT mice after 4 weeks of AB surgery (Figure 3F). Quantitative analysis of
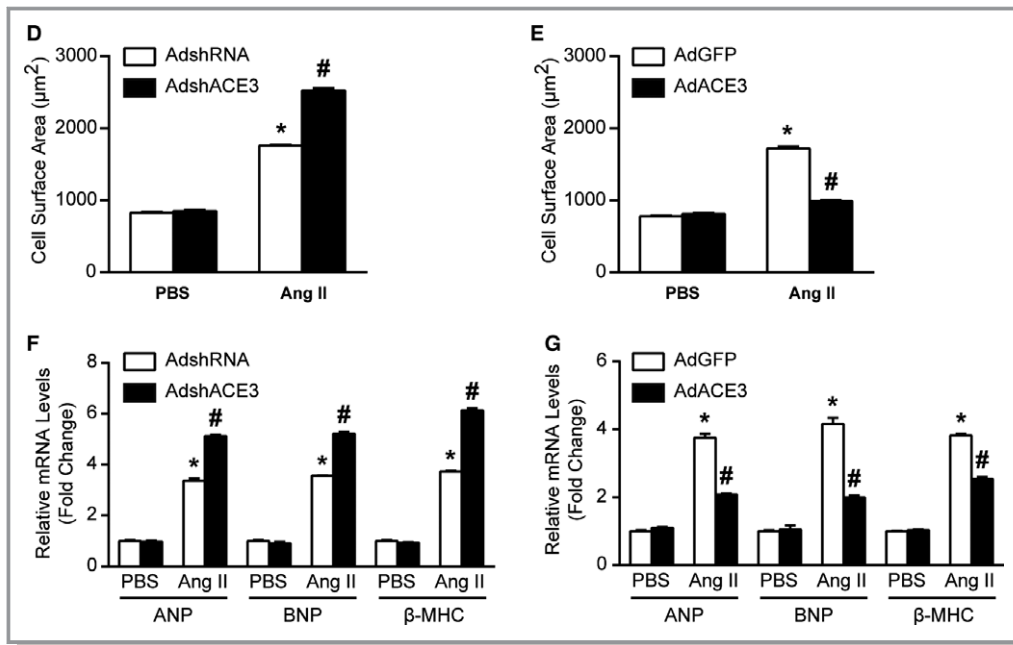
Figure 2. Continued.

the left ventricular (LV) collagen volume is shown in Figure 3G. These results were further corroborated by detecting the mRNA levels of fibrotic markers (ie, collagen I, collagen III, and fibronectin) which indicated an augmented fibrotic response in the ACE3-KO hearts (Figure 3I). Together, these data provide evidence that ACE3 deficiency accentuates pathological cardiac remodeling upon chronic pressure overload.

Overexpression of ACE3 Attenuates Cardiac Hypertrophy Induced by Pressure Overload

Next, to determine whether ACE3 overexpression could attenuate pressure overload-induced cardiac hypertrophy and remodeling, transgenic (TG) mice with cardiac-specific overexpression of ACE3 were generated using the CAG promoter (Figure 4A). Four dependent ACE3-TG mouse lines were established, and western blotting analysis revealed that ACE3 expression in the different lines was increased more than 2-folds in relative to the CAG-CAT-mACE3/α-MHC-MerCreMer mice without tamoxifen administration (CAMC) littermates (Figure 4B). We chose the TG3 mouse line which had the highest expression of ACE3, for use in the following experiments. As shown in Figure 4C, AB induced obvious cardiac hypertrophy in CAMC mice, which was evidenced by the ratios of HW/BW, LW/BW, and HW/TL. There were no apparent differences in the sham operation groups between ACE3-TG mice and CAMC mice, whereas the ACE3-TG mice showed significant blunted hypertrophic response upon AB surgery. Similarly, histological analyses revealed that the

cardiomyocyte cross-sectional area was decreased by ≈23% in AB-operated ACE3-TG mice compared with CAMC mice (Figure 4D and 4E). The hallmarks of cardiac hypertrophy, ANP, BNP and β-MHC, were also suppressed significantly in AB-operated ACE3-TG mice (Figure 4I). These results were consistent with the protective role of ACE3 in cardiac contractile function in response to hypertrophic stress. As indicated by LVEDd, LVESd, and FS, the cardiac contractile function was improved remarkably in ACE3-TG mice compared with CAMC mice (Figure 4F). Furthermore, histological analysis and the analyses of fibrotic markers cooperatively demonstrated a decreased fibrotic response in the AB-operated ACE3-TG mice compared with the AB-operated CAMC mice (Figure 4G, 4H, and 4J). Collectively, these data indicate that ACE3 overexpression attenuates pathological cardiac hypertrophy, fibrosis, and dysfunction in response to pressure overload.

Effect of ACE3 on MEK-ERK1/2 Signaling Pathway In Vitro and In Vivo

To understand the molecular mechanisms through which decreased ACE3 enhances the hypertrophic response, both AdACE3- and AdshACE3-infected NRCMs were exposed to 1 μmol/L Ang II or PBS control for 60 minutes to examine the potential signaling molecules. Substantial evidence has suggested that the mitogen-activated protein kinase (MAPK) signaling pathway plays an important role in the development of cardiac hypertrophy.[15,16] Using western blotting, we found that the phosphorylated levels of MEK1/2 and ERK1/2 were
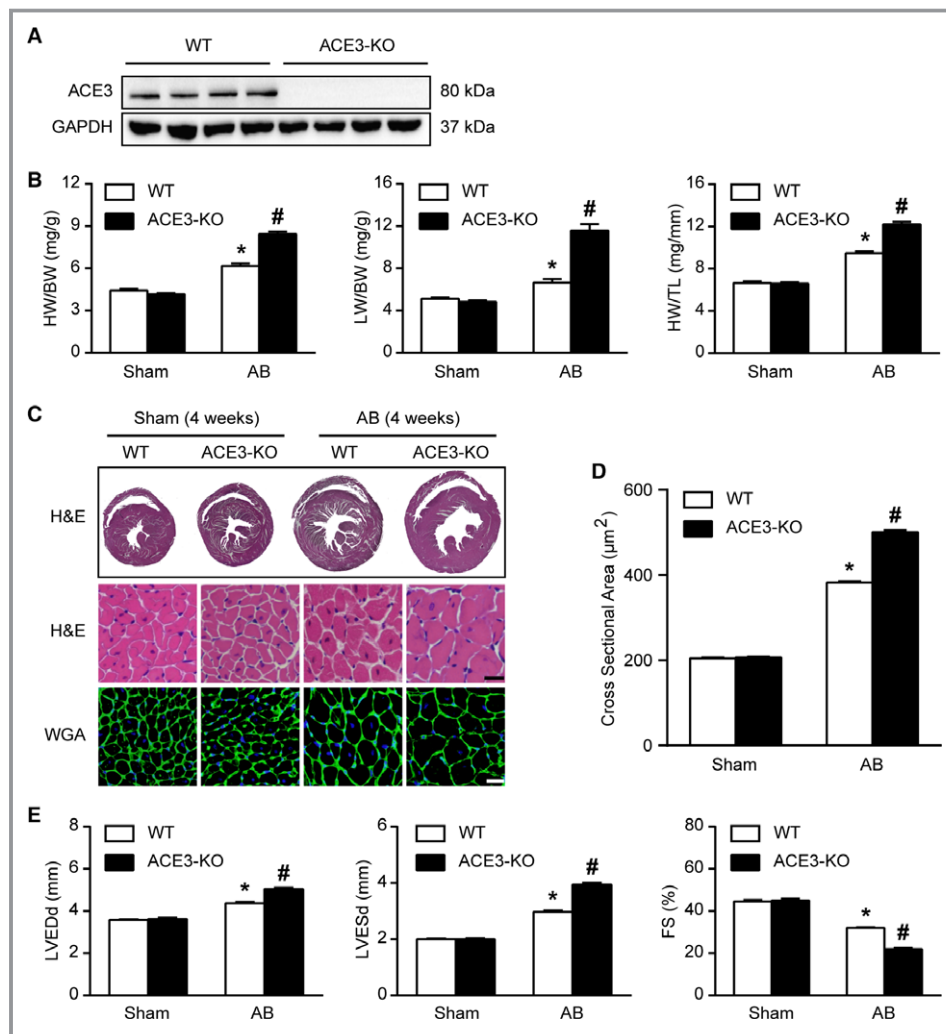
Figure 3. Angiotensin-converting enzyme 3 knockout (ACE3-KO) aggravates pressure overload-induced cardiac hypertrophy. A, Western blot analysis for ACE3 in heart tissues of WT and ACE3-KO mice (n=4 mice in each group). B, The results for the ratios of HW/BW, LW/BW, and HW/TL in WT and ACE3-KO mice 4 weeks after sham operation or AB surgery (n=12 mice in each group). C, Histological sections of hearts from WT and ACE3-KO mice subjected to AB or sham operation were stained with hematoxylin & eosin (H&E) and wheat germ agglutinin (WGA) to analyze heart and cardiomyocyte size (n=6 mice in Sham group and 5 mice in AB group; scale bars, 20 μm). D, The results for the cross-sectional area of cardiomyocytes (n=100+ cells in each group). E, Parameters of the echocardiographic results (LVEDd, LVESd, and FS) for the indicated groups (n=7 mice in each group). F, Picrosirius red (PSR) staining of histological sections of the left ventricle (LV) in the WT and ACE3-KO mice 4 weeks after sham or AB treatment (n=6 mice in Sham group and 5 mice in AB group; scale bars, 50 μm). G, Quantification of the total collagen volume in the indicated groups (n=25+ fields in each group). H and I, Real-time PCR analyses of hypertrophic markers (ANP, BNP, and β-MHC) and fibrotic markers (collagen I, collagen III, and fibronectin) in the hearts of WT and ACE3-KO mice 4 weeks after sham operation or AB surgery (n=4 mice in each group). LVEDd indicates LV end-diastolic diameter; LVESd, LV-end systolic diameter; FS, fractional shortening. *$P<0.05$ vs WT/sham; #$P<0.05$ vs WT/AB.

significantly increased in Ang II-treated AdshRNA-infected NRCMs and were further markedly enhanced by AdshACE3 infection (Figure 5A). However, P38 and c-Jun N-terminal kinase 1/2 (JNK1/2) were similarly activated in 2 groups. Our further studies showed that the Ang II-induced activation of MEK and ERK1/2 was almost completely blocked by infection with AdACE3 (Figure 5B). Collectively, these findings suggest that although the altered expression levels of ACE3 had no effects on P38 and JNK1/2 activation in hearts subjected to Ang II treatment, the upregulation of ACE3 blunted the
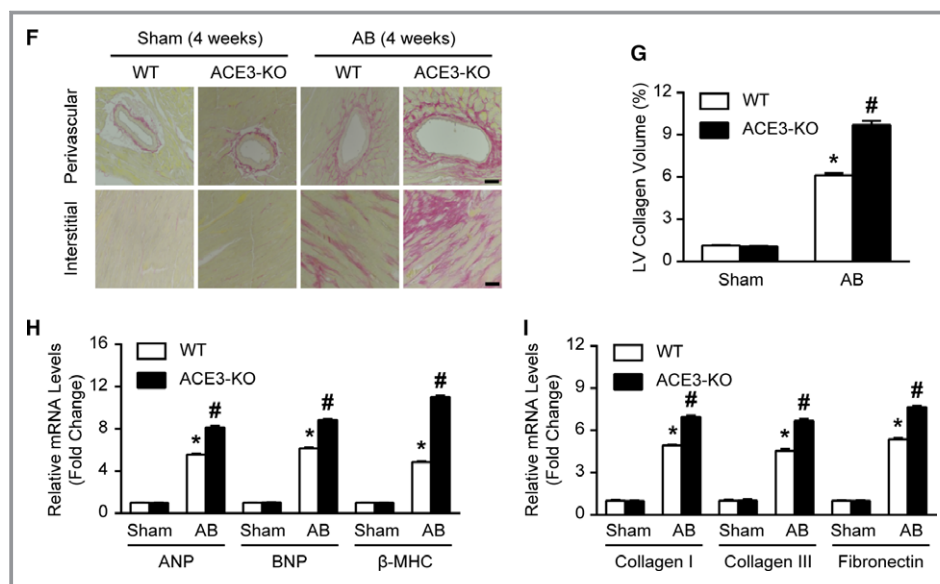
Figure 3. Continued.

activation of the MEK–ERK1/2 signaling, whereas the down-regulation of ACE3 enhanced MEK–ERK1/2 activation. To further elucidate the functional role played by MEK-ERK1/2 signaling in the hypertrophy-attenuating function of ACE3 in vivo, we treated ACE3-KO and ACE3-TG mice with 4 weeks of AB. As expected, the chronic pressure overload-induced activation of MEK and ERK1/2 were significantly increased in the ACE3-deficient mouse hearts; however, these activations were almost completely blocked by ACE3 overexpression (Figure 5C and 5D). Together, our in vitro and in vivo results suggest that the inhibitory effect of ACE3 against cardiac hypertrophy may be ascribed to direct inhibition of the MEK-ERK1/2 signaling.

Inhibition of the MEK–ERK1/2 Signaling Pathway Rescues Abnormalities in ACE3-KO Mice

We have provided evidence that ACE3 inhibits pathological cardiac hypertrophy through blocking MEK-ERK1/2-dependent signaling pathways. To further confirm these findings, we evaluated whether inhibiting this signaling pathway could reverse the abnormalities in ACE3-KO mice. We treated the ACE3-KO mice with U0126 (a specific MEK1/2 inhibitor) or DMSO dissolved in saline solution 4 weeks after AB surgery. The western blots showed that the phosphorylation levels of MEK and ERK1/2 were almost completely abrogated in the U0126-treated mice compared with DMSO-treated control mice (Figure 6A). U0126 treatment significantly reversed the deteriorative effects on cardiac and myocytes morphology, cardiac function, and fibrosis in response to AB surgery compared with DMSO treatment in ACE3-KO mice (Figure 6B

through 6G). These findings suggest that pharmacological inhibition of the MEK–ERK1/2 signaling could neutralize the pro-hypertrophic effects in the ACE3-deficient mice hearts upon pressure overload.

Discussion

Pathological hypertrophy is ultimately a detrimental process that is associated with malignant arrhythmia and heart failure.[1] Therefore, identifying efficient targets to suppress of maladaptive hypertrophy may be a useful therapeutic strategy to prevent heart failure and other heart related diseases. Our present study, using both gain- and loss-of-function approaches revealed that loss of ACE3 rendered mice more prone to pressure overload-induced cardiac hypertrophy, fibrosis, and dysfunction, conversely, ACE3 overexpression protected against pathological hypertrophy. Mechanistically, we demonstrated that ACE3 displayed an anti-hypertrophic effect through targeted inhibition of the MEK-ERK1/2 signaling. Therefore, we provide the first evidence suggesting that ACE3 is an important modulator of the development of pathological cardiac hypertrophy.

ACE3 belongs to the mammalian ACE family which consists of 3 members: ACE, ACE2, and ACE3. In addition to the well-characterized ACE-mediated regulation of blood pressure and cardiovascular homeostasis, previous studies have demonstrated a critical protective role for ACE2 in response to different cardiac pathologies.[17,18] Considering the structural similarity between ACE3 and the existing members of the ACE family and the growing evidence from the authenticated beneficial effects of ACE2, it will be
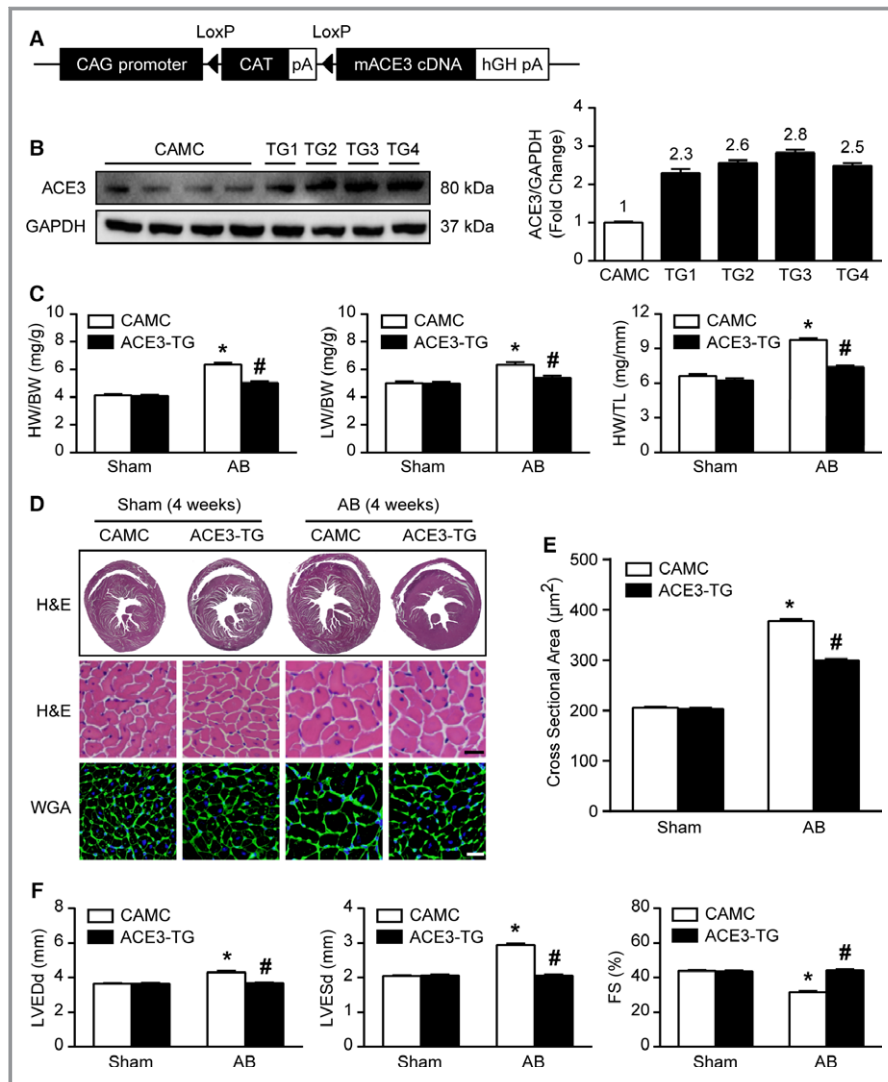
Figure 4. Angiotensin-converting enzyme 3 (ACE3) overexpression attenuates pressure overload-induced cardiac hypertrophy. A, Schematic diagram depicting the construct that used to generate ACE3-transgenic (TG) mouse lines. B, Cardiac ACE3 expression in TG mice and their CAG-CAT-mACE3/α-MHC-MerCreMer mice without tamoxifen administration (CAMC) littermates (n=3 independent experiments). C, The results for the ratios of HW/BW, LW/BW, and HW/TL in CAMC and ACE3-TG mice 4 weeks after sham operation or AB surgery (n=13 mice in Sham group and 12 mice in AB group). D, Histological sections of hearts from CAMC and ACE3-TG mice subjected to AB or sham operation were stained with hematoxylin & eosin (H&E) and wheat germ agglutinin (WGA) to analyze heart and cardiomyocyte size (n=6 mice in Sham group and 5 mice in AB group; scale bars, 20 μm). E, The results for the cross-sectional area of cardiomyocytes (n=100+ cells in each group). F, Parameters of the echocardiographic results (LVEDd, LVESd, and FS) for the indicated groups (n=8 mice in Sham group and 7 mice in AB group). G, PSR staining of histological sections of the LV in the CAMC and ACE3-TG mice 4 weeks after AB or sham treatment (n=6 mice in Sham group and 5 mice in AB group; scale bars, 50 μm). H, Quantification of the total collagen volume in the indicated groups (n=25+ fields in each group). I and J, Real-time PCR analyses of the hypertrophic markers (ANP, BNP, and β-MHC) and fibrotic markers (collagen I, collagen III, and fibronectin) in the hearts of CAMC and ACE3-TG mice 4 weeks after sham operation or AB surgery (n=4 mice in each group). *$P<0.05$ vs CAMC/sham; #$P<0.05$ vs CAMC/AB.

interesting to determine whether ACE3 possesses a functional role in different cardiovascular pathologies, especially in the development of pathological cardiac hypertrophy. Ang II is

thought to be involved in almost all of the important processes of pathological cardiac hypertrophy, including myocyte hypertrophy, fetal gene reprogramming, fibroblast
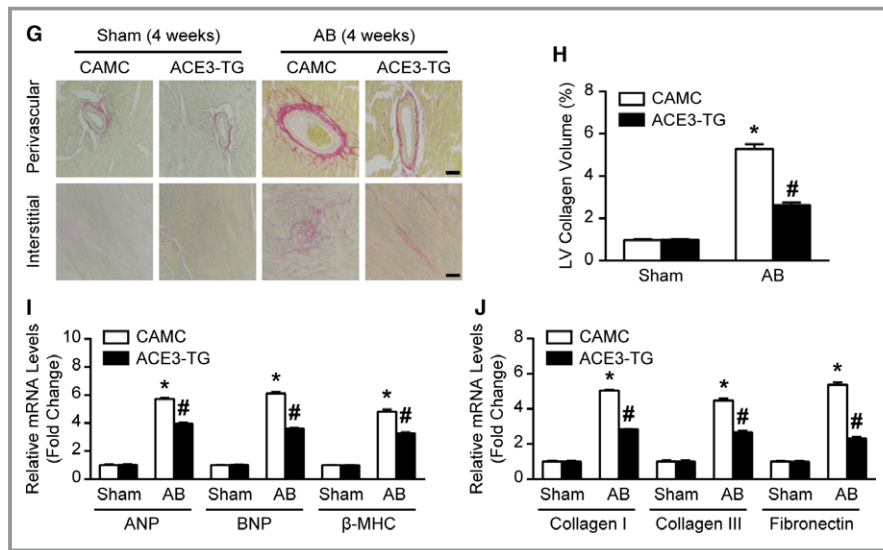
Figure 4. Continued.

proliferation, and accumulation of ECM protein.[19] Therefore, interventions affecting the production or function of Ang II may provide beneficial effects toward cardiovascular pathology. In the current study, we first tested the expression levels of ACE3 during Ang II-induced cardiomyocyte hypertrophy and we found that ACE3 expression was decreased in Ang II-treated NRCMs. These findings indicated a potential role for ACE3 in the regulation of pathological cardiac hypertrophy. Then, our in vitro experiments demonstrated that ACE3 can limit the hypertrophic growth of NRCMs in response to Ang II stimulation. Consistent with this, further in vivo studies using genetically engineered mice also found that ACE3 provides protective effects against chronic pressure overload-induced cardiac hypertrophy, fibrosis, and dysfunction. Accumulating evidence has pointed out that ACE2 and its primary product Ang 1 to 7 play critical roles in the pathophysiology of cardiovascular disease, especially the protective actions against pathological cardiac hypertrophy.[20,21] We demonstrated that ACE3, as a new component of the ACE family, has the ability to impair Ang II- and pressure overload-induced cardiac hypertrophy in this study. Although ACE3 shares the structural similarity with ACE2, Monika et al[8] have pointed out that several substitutions occur in the predicted ACE3 active site, including the most important Glu residue that conserved in ACE family. This suggests that ACE3 will not be a functional protease that catalyzes the proteolysis of Ang II and the production of Ang 1 to 7. Moreover, we found that downregulation or upregulation of ACE3 in NRCMs did not affect the gene expression level of ACE2. Taken together, it appears that the inhibitory effects of ACE3 on cardiac hypertrophy are not dependent on the regulation of Ang II and the production of Ang 1 to 7.

Extensive studies have targeted the activation status of the MAPK signaling during the development of pathological cardiac hypertrophy. This signaling cascade is initiated by a sequence of successively functional kinases and ultimately results in activation of 3 main protein kinases: p38, JNKs and ERKs.[22] Among these 3 kinases, activation of ERK1/2 is thought to be involved in virtually every characterized hypertrophic stimulus in vitro and in vivo investigations.[23] In our present study, ACE3 overexpression markedly attenuated the hypertrophic phenotype in response to pressure overload, and the activation of MEK-ERK1/2 signaling was almost completely eliminated. However, augmented activation of the MEK-ERK1/2 signaling was found in ACE3 deficiency-mediated aggravated pressure overload-induced cardiac hypertrophy. Meanwhile, pharmacological inhibition of MEK-ERK1/2 signaling rescued cardiac dysfunction and remodeling in ACE3-deficient mice subjected to chronic pressure overload. All of these results suggest that ACE3 alleviates cardiac hypertrophy, at least in part, via inhibition of the MEK-ERK1/2 signaling. Our present findings are also consistent with the ability of the increased activation of MEK-ERK1/2 signaling to exacerbate the pathological cardiac hypertrophy observed in other studies. Previous studies have demonstrated that the antagonistic roles of ACE2 on the worsening cardiac fibrosis and pathological hypertrophy were associated with the inhibition of the ERK1/2 signaling activity, which was markedly increased in ACE2-deficient mice in response to pressure overload.[20] Carabin, a protein expressed mainly in the immune system and the heart, was shown as a negative regulator of cardiac hypertrophy that induced by pressure overload and adrenergic stimulation, partly though inhibition of the MEK-ERK1/2 signaling.[24] Since we have validated the
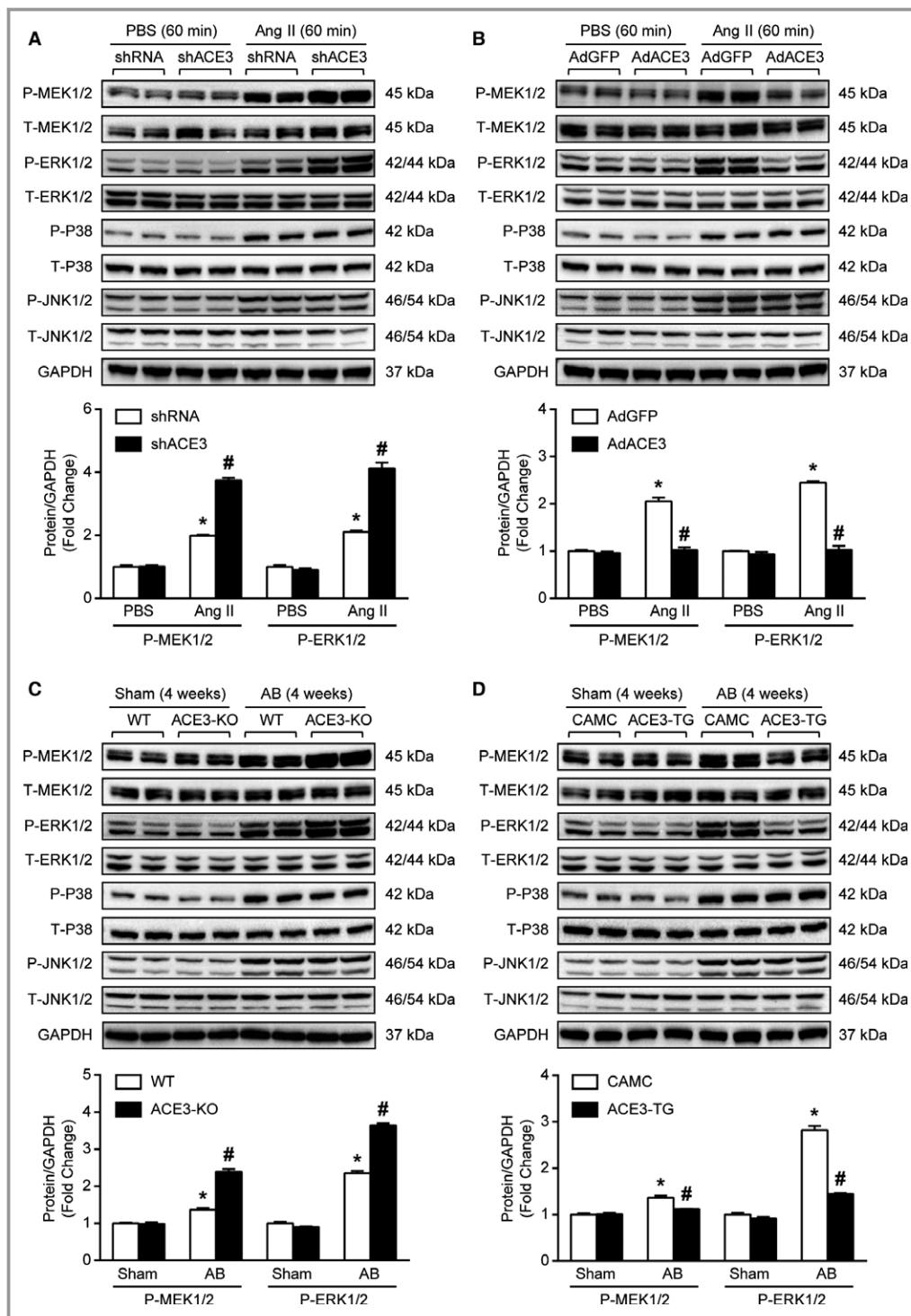
Figure 5. Effect of angiotensin-converting enzyme 3 (ACE3) on MEK-ERK1/2 signaling pathway. A and B, Top: Representative western blots of MEK1/2, ERK1/2, P38, and JNK1/2 phosphorylation and total protein levels in NRCMs infected with AdshACE3 or AdACE3 after 60 minutes of PBS or Ang II treatment. Bottom: Quantification results of P-MEK and P-ERK1/2 expression levels in the indicated groups (n=6 samples in each group; *P<0.05 vs AdshRNA/PBS or AdGFP/PBS; #P<0.05 vs AdshRNA/Ang II or AdGFP/Ang II). C and D, Top: Representative western blots of MEK1/2, ERK1/2, P38, and JNK1/2 phosphorylation and total protein levels in hearts from ACE3-KO and ACE3-TG mice at 4 weeks after sham operation or AB surgery. Bottom: Quantification results of P-MEK and P-ERK1/2 expression levels in the indicated groups (n=6 mice in each group; *P<0.05 vs WT/sham or CAMC/sham; #P<0.05 vs WT/AB or CAMC/AB).
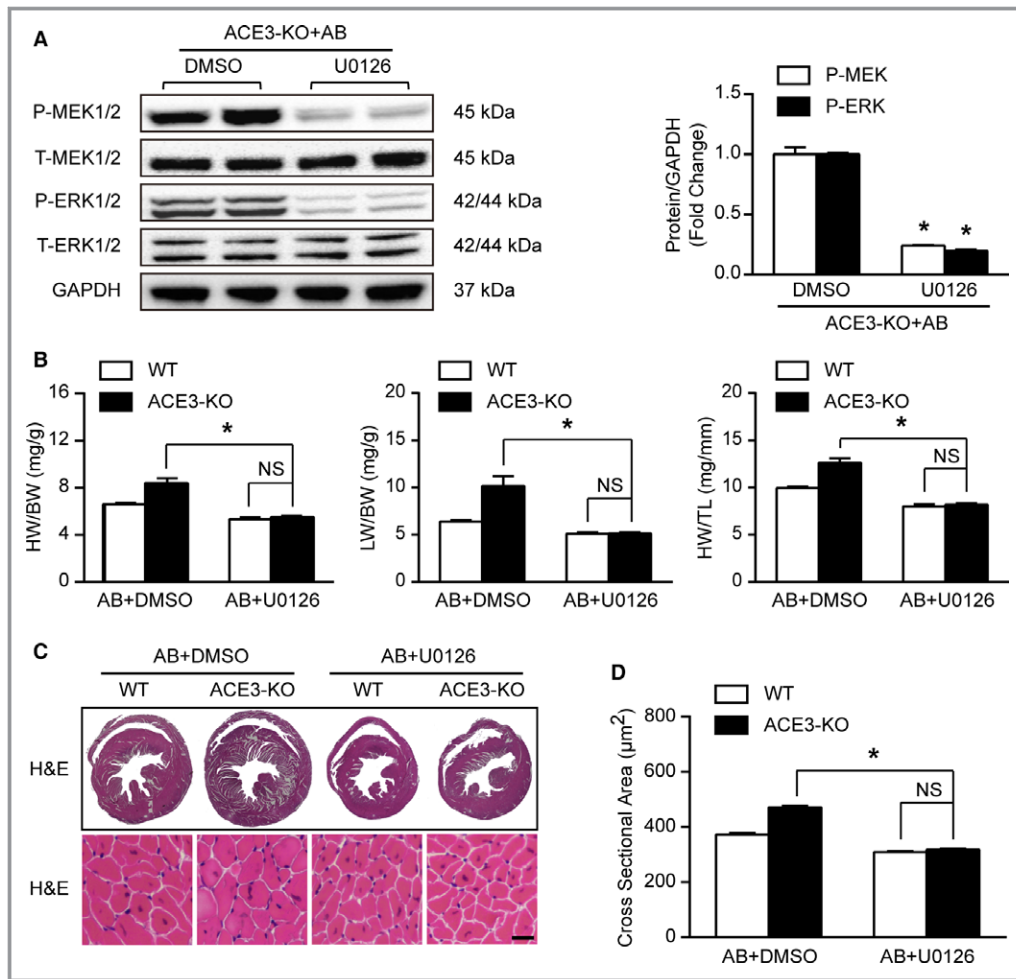
Figure 6. Inhibition of MEK-ERK1/2 signaling rescues abnormalities in angiotensin-converting enzyme 3–knockout (ACE3-KO) mice. A, U0126 blocked MEK1/2 and ERK1/2 phosphorylation 4 weeks after AB surgery in ACE3-KO mice (n=3 independent experiments; *P<0.05 vs DMSO, respectively). B, The results for the ratios of HW/BW, LW/BW, and HW/TL in WT and ACE3-KO mice 4 weeks after AB surgery and treatment with U0126 (n=8 mice in each group; *P<0.05; and NS, no significance). C, Histological analyses of HE staining in the indicated groups (n=4 mice in each group; scale bar, 20 mm). D, Results for the ratios of cell sectional area in the indicated groups (n=100+ cells per experimental group; *P<0.05; and NS, no significance). E, Parameters of the echocardiographic results (LVEDd, LVESd, and FS) in WT and ACE3-KO mice at 4 weeks after AB surgery and treatment with U0126. (n=6 mice in ACE3-KO/AB+DMSO group and 8 mice in other groups; *P<0.05; and NS, no significance). F, PSR staining of histological sections of the LV in the indicated groups (n=4 mice in each group; scale bars, 50 μm). G, Quantification of the total collagen volume in the indicated groups (n=25+ fields in each group; *P<0.05; and NS, no significance).

protective roles of ACE3 in response to Ang II- and pressure overload-induced cardiac hypertrophy, it has significance to test whether ACE3 can also affect other types of cardiac hypertrophy, such as the adrenergic receptor-induced cardiac hypertrophy. Among the multiple signaling pathways that activated by the adrenergic receptors, a large body of evidence has showed the essential roles of the ERK1/2 signaling during different adrenergic receptor-induced hypertrophic response.[25,26] As we have demonstrated the anti-hypertrophic effects of ACE3 are mainly depend on inhibition of the MEK-ERK1/2 signaling, it is likely that ACE3 can also

function as a negative regulator in adrenergic receptor-induced hypertrophy. However, further study should be performed to validate this assumption.

The limitation of this study was that the mechanisms regarding the regulation of ACE3 expression pattern were not examined. However, the mechanisms can be hypothesized based on the studies about the expression changes of other members of the ACE family during Ang II stimulation. Patricia et al[27] have demonstrated that the Ang II type 1 receptor (AT1R)-mediated ERK1/2 signaling pathway is a critical mechanism by which Ang II downregulates the expression
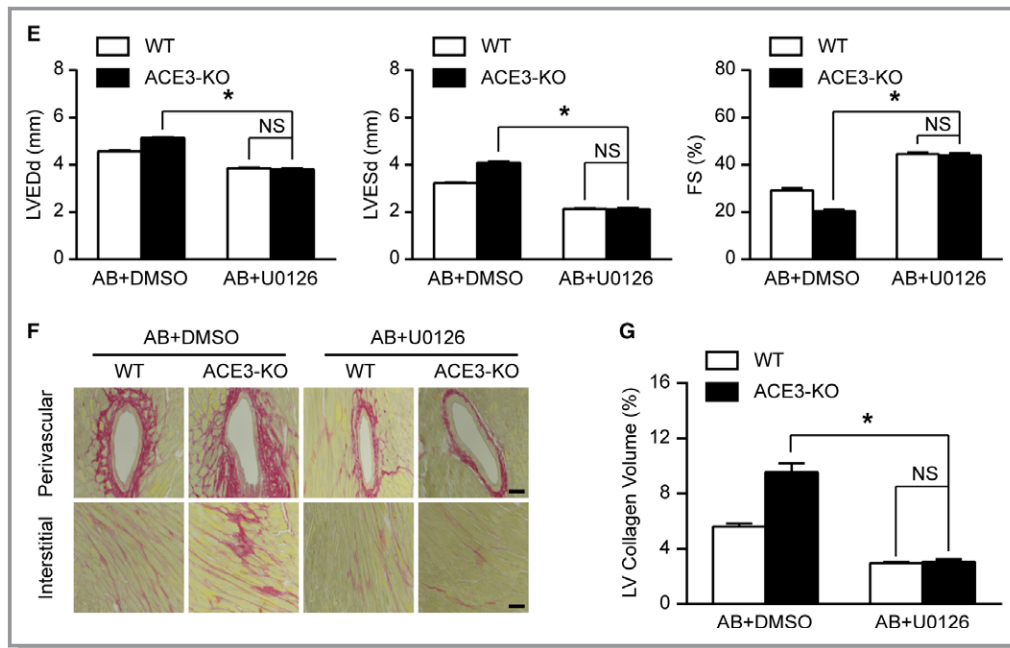
Figure 6. Continued.

levels of ACE2 in cardiomyocytes. Other studies using different cell models also found that Ang II upregulates ACE but downregulates ACE2 expression through the p38 MAPK and ERK1/2 signaling pathway.[28,29] Therefore, we can speculate that the MAPK signaling may be involved in the regulation of the expression of ACE3 upon Ang II stimulation. However, additional studies are required to confirm this hypothesis.

In conclusion, the findings from our present work provide the first evidence that ACE3 inhibits the development of pathological cardiac hypertrophy both in vitro and in vivo, at least in part, through suppressing the MEK-ERK1/2 signaling pathway. These observations broaden our understanding of the functional roles of ACE3 in certain pathological condition and provide new insights into the mechanisms of the development of cardiac hypertrophy.

Acknowledgments

Sources of Funding

Disclosures

None.

References

1. Frey N, Katus HA, Olson EN, Hill JA. Hypertrophy of the heart: a new therapeutic target? *Circulation*. 2004;109:1580–1589.

2. Levy D, Garrison RJ, Savage DD, Kannel WB, Castelli WP. Prognostic implications of echocardiographically determined left ventricular mass in the Framingham Heart Study. *N Engl J Med*. 1990;322:1561–1566.

3. Koren MJ, Devereux RB, Casale PN, Savage DD, Laragh JH. Relation of left ventricular mass and geometry to morbidity and mortality in uncomplicated essential hypertension. *Ann Intern Med*. 1991;114:345–352.

4. Koitabashi N, Kass DA. Reverse remodeling in heart failure–mechanisms and therapeutic opportunities. *Nat Rev Cardiol*. 2012;9:147–157.

5. Jiang DS, Wei X, Zhang XF, Liu Y, Zhang Y, Chen K, Gao L, Zhou H, Zhu XH, Liu PP, Bond Lau W, Ma X, Zou Y, Zhang XD, Fan GC, Li H. IRF8 suppresses pathological cardiac remodelling by inhibiting calcineurin signalling. *Nat Commun*. 2014;5:3303.

6. Li H, He C, Feng J, Zhang Y, Tang Q, Bian Z, Bai X, Zhou H, Jiang H, Heximer SP, Qin M, Huang H, Liu PP, Huang C. Regulator of G protein signaling 5 protects against cardiac hypertrophy and fibrosis during biomechanical stress of pressure overload. *Proc Natl Acad Sci USA*. 2010;107:13818–13823.

7. Zhang XJ, Zhang P, Li H. Interferon regulatory factor signalings in cardiometabolic diseases. *Hypertension*. 2015;66:222–247.

8. Rella M, Elliot JL, Revett TJ, Lanfear J, Phelan A, Jackson RM, Turner AJ, Hooper NM. Identification and characterisation of the angiotensin converting enzyme-3 (ACE3) gene: a novel mammalian homologue of ACE. *BMC Genomics*. 2007;8:194.

9. Inoue N, Kasahara T, Ikawa M, Okabe M. Identification and disruption of sperm-specific angiotensin converting enzyme-3 (ACE3) in mouse. *PLoS One*. 2010;5:e10301.

10. Jiang DS, Bian ZY, Zhang Y, Zhang SM, Liu Y, Zhang R, Chen Y, Yang Q, Zhang XD, Fan GC, Li H. Role of interferon regulatory factor 4 in the regulation of pathological cardiac hypertrophy. *Hypertension*. 2013;61:1193–1202.

11. Jiang DS, Luo YX, Zhang R, Zhang XD, Chen HZ, Zhang Y, Chen K, Zhang SM, Fan GC, Liu PP, Liu DP, Li H. Interferon regulatory factor 9 protects against cardiac hypertrophy by targeting myocardin. *Hypertension*. 2014;63:119–127.

12. Jiang DS, Li L, Huang L, Gong J, Xia H, Liu X, Wan N, Wei X, Zhu X, Chen Y, Chen X, Zhang XD, Li H. Interferon regulatory factor 1 is required for cardiac remodeling in response to pressure overload. *Hypertension*. 2014;64:77–86.

13. Lu J, Bian ZY, Zhang R, Zhang Y, Liu C, Yan L, Zhang SM, Jiang DS, Wei X, Zhu XH, Chen M, Wang AB, Chen Y, Yang Q, Liu PP, Li H. Interferon regulatory factor 3 is a negative regulator of pathological cardiac hypertrophy. *Basic Res Cardiol*. 2013;108:326.

14. Jiang DS, Zhang XF, Gao L, Zong J, Zhou H, Liu Y, Zhang Y, Bian ZY, Zhu LH, Fan GC, Zhang XD, Li H. Signal regulatory protein-alpha protects against cardiac hypertrophy via the disruption of toll-like receptor 4 signaling. *Hypertension*. 2014;63:96–104.

15. Muslin AJ. MAPK signalling in cardiovascular health and disease: molecular mechanisms and therapeutic targets. *Clin Sci (Lond)*. 2008;115:203–218.

16. Rose BA, Force T, Wang Y. Mitogen-activated protein kinase signaling in the heart: angels versus demons in a heart-breaking tale. *Physiol Rev*. 2010;90:1507–1546.

17. Yamamoto K, Ohishi M, Katsuya T, Ito N, Ikushima M, Kaibe M, Tatara Y, Shiota A, Sugano S, Takeda S, Rakugi H, Ogihara T. Deletion of angiotensin-converting enzyme 2 accelerates pressure overload-induced cardiac dysfunction by increasing local angiotensin II. *Hypertension*. 2006;47:718–726.

18. Dong B, Yu QT, Dai HY, Gao YY, Zhou ZL, Zhang L, Jiang H, Gao F, Li SY, Zhang YH, Bian HJ, Liu CX, Wang N, Xu H, Pan CM, Song HD, Zhang C, Zhang Y. Angiotensin-converting enzyme-2 overexpression improves left ventricular remodeling and function in a rat model of diabetic cardiomyopathy. *J Am Coll Cardiol*. 2012;59:739–747.

19. Kim S, Iwao H. Molecular and cellular mechanisms of angiotensin II-mediated cardiovascular and renal diseases. *Pharmacol Rev*. 2000;52:11–34.

20. Zhong J, Basu R, Guo D, Chow FL, Byrns S, Schuster M, Loibner H, Wang XH, Penninger JM, Kassiri Z, Oudit GY. Angiotensin-converting enzyme 2 suppresses pathological hypertrophy, myocardial fibrosis, and cardiac dysfunction. *Circulation*. 2010;122:717–728, 718 p following 728.

21. McCollum LT, Gallagher PE, Ann Tallant E. Angiotensin-(1-7) attenuates angiotensin II-induced cardiac remodeling associated with upregulation of dual-specificity phosphatase 1. *Am J Physiol Heart Circ Physiol*. 2012;302:H801–H810.

22. van Berlo JH, Maillet M, Molkentin JD. Signaling effectors underlying pathologic growth and remodeling of the heart. *J Clin Invest*. 2013;123:37–45.

23. Bueno OF, Molkentin JD. Involvement of extracellular signal-regulated kinases 1/2 in cardiac hypertrophy and cell death. *Circ Res*. 2002;91:776–781.

24. Bisserier M, Berthouze-Duquesnes M, Breckler M, Tortosa F, Fazal L, de Regibus A, Laurent AC, Varin A, Lucas A, Branchereau M, Marck P, Schickel JN, Delomenie C, Cazorla O, Soulas-Sprauel P, Crozatier B, Morel E, Heymes C, Lezoualc'h F. Carabin protects against cardiac hypertrophy by blocking calcineurin, Ras, and Ca^{2+}/calmodulin-dependent protein kinase II signaling. *Circulation*. 2015;131:390–400; discussion 400

25. Zhong L, Chiusa M, Cadar AG, Lin A, Samaras S, Davidson JM, Lim CC. Targeted inhibition of ANKRD1 disrupts sarcomeric ERK-GATA4 signal transduction and abrogates phenylephrine-induced cardiomyocyte hypertrophy. *Cardiovasc Res*. 2015;106:261–271.

26. Taglieri DM, Monasky MM, Knezevic I, Sheehan KA, Lei M, Wang X, Chernoff J, Wolska BM, Ke Y, Solaro RJ. Ablation of p21-activated kinase-1 in mice promotes isoproterenol-induced cardiac hypertrophy in association with activation of Erk1/2 and inhibition of protein phosphatase 2A. *J Mol Cell Cardiol*. 2011;51:988–996.

27. Gallagher PE, Ferrario CM, Tallant EA. Regulation of ACE2 in cardiac myocytes and fibroblasts. *Am J Physiol Heart Circ Physiol*. 2008;295:H2373–H2379.

28. Xiao L, Haack KK, Zucker IH. Angiotensin II regulates ACE and ACE2 in neurons through p38 mitogen-activated protein kinase and extracellular signal-regulated kinase 1/2 signaling. *Am J Physiol Cell Physiol*. 2013;304:C1073–C1079.

29. Koka V, Huang XR, Chung AC, Wang W, Truong LD, Lan HY. Angiotensin II up-regulates angiotensin I-converting enzyme (ACE), but down-regulates ACE2 via the AT1-Erk/p38 MAP kinase pathway. *Am J Pathol*. 2008;172:1174–1183.